

EFFECTS ON THE ENERGY FLUX DENSITY DUE TO PITCH IN TWISTED CLAD OPTICAL FIBERS

Muhammad A. Baqir and Pankaj K. Choudhury*

Institute of Microengineering and Nanoelectronics, Universiti Kebangsaan Malaysia, UKM Bangi, Selangor 43600, Malaysia

Abstract—The paper deals with the propagation of electromagnetic waves through twisted clad dielectric optical fibers. The structure of these fibers is analogous to travelling wave tubes used in microwave devices, and the usefulness would be in the areas of optical sensing. This is because the twists in fiber would be affected due to the imposed stress and/or strain, leaving thereby the possibility to alter the propagation characteristics. A rigorous analytical investigation has been carried out with the emphasis on the energy flux density patterns due to the different propagating modes in the fiber. The dispersion relations of the system are deduced and the energy flux densities are evaluated under different pitch angles of twist. The effect due to conducting helix pitch on the electromagnetic wave propagation is emphasized.

1. INTRODUCTION

The usefulness of optical waveguides has been obvious in varieties of applications that include the areas related to optical communications, photonics and integrated optical devices. During the last couple of decades, considerable amount of investigations have been reported, by taking into account varieties of guides with different structures and compositions [1–17]. Within the context, twisted clad optical fiber is of special type in which the fiber core is bounded with conducting helical windings [18–20]. These are complex guiding structures wherein the pitch angle of twists (at the core-clad boundary) is used to tailor the dispersion behavior as well as the energy flux density corresponding to different sustained modes.

Twisted structures are commonly implemented in travelling wave tubes (TWTs) for microwave generation [21]. The use of these in

Received 11 April 2013, Accepted 10 May 2013, Scheduled 13 May 2013

* Corresponding author: Pankaj Kumar Choudhury (pankaj@ukm.my).

the case of cylindrical and elliptical dielectric optical fibers have been reported in the literature [18–20]. To a more complex stage, studies of chiral and liquid crystal fibers with a loading of twisted conducting structures at the core-clad interface have been presented [22, 23].

Investigations of twisted clad cylindrical and/or elliptical structures reported so far have been limited to the estimation of dispersion characteristics of the guide and the effects due to varying pitch angles. However, the flux density characteristics of these guides have not yet been given enough attention. In the present communication, we aim to study the energy flux density patterns corresponding to the sustained modes in dielectric cylindrical core waveguides with conducting helical windings. The eigenvalue equations of the guide are deduced corresponding to the situations of parallel and perpendicular orientations of the sheath helical wraps with respect to the optical axis of the guide, which give information about the sustained modes. Energy flux density patterns propagating through the guide are then evaluated based on the effects due the loaded helix pitch angle.

2. THEORY

We consider a dielectric step-index optical fiber having circular cross-section having radius a , which is loaded with conducting sheath helical windings at the core-clad interface, as shown in Fig. 1. In this connection, it must be noted that these conducting helical turns are tightly bound, but still insulated from each other. The refractive index (RI) values of core and the infinitely extended clad sections are n_1 and n_2 , respectively, and the optical axis of fiber is aligned to the z -direction. Also, ψ represents the pitch angle of helix, i.e., the

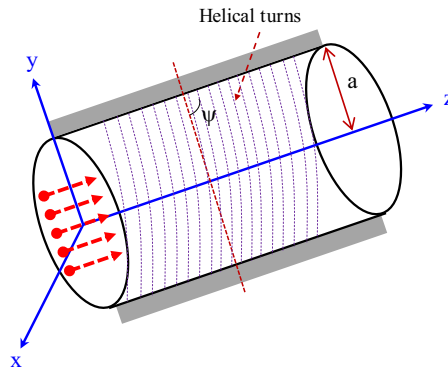


Figure 1. Schematic of the twisted clad fiber.

angle that conducting helical turns make with the optical axis of fiber. Considering the time t - and axis z -harmonic waves to propagate in the fiber, the transverse and the longitudinal components of fields in the core/clad regions may be obtained [24] as follows:

$$E_{r1} = -\frac{j}{u^2} \left\{ A_1 \beta u J'_\nu(ur) + j \frac{\omega \mu \nu}{r} B_1 J_\nu(ur) \right\} e^{j(\omega t - \beta z + \nu \phi)} \quad (1a)$$

$$H_{r1} = \frac{j}{u^2} \left\{ j \frac{\omega \varepsilon \nu}{r} A_1 J_\nu(ur) - \beta u B_1 J'_\nu(ur) \right\} e^{j(\omega t - \beta z + \nu \phi)} \quad (1b)$$

$$E_{\phi 1} = -\frac{j}{u^2} \left\{ j \frac{\beta \nu}{r} A_1 J_\nu(ur) - \omega \mu u B_1 J'_\nu(ur) \right\} e^{j(\omega t - \beta z + \nu \phi)} \quad (2a)$$

$$H_{\phi 1} = -\frac{j}{u^2} \left\{ \omega \varepsilon u A_1 J'_\nu(ur) + j \frac{\beta \nu}{r} B_1 J_\nu(ur) \right\} e^{j(\omega t - \beta z + \nu \phi)} \quad (2b)$$

$$E_{r2} = -\frac{j}{w^2} \left\{ C_1 \beta w K'_\nu(wr) + j \frac{\omega \mu \nu}{r} D_1 K_\nu(wr) \right\} e^{j(\omega t - \beta z + \nu \phi)} \quad (3a)$$

$$H_{r2} = \frac{j}{w^2} \left\{ j \frac{\omega \mu \nu}{r} C_1 K_\nu(wr) - \beta w D_1 K'_\nu(wr) \right\} e^{j(\omega t - \beta z + \nu \phi)} \quad (3b)$$

$$E_{\phi 2} = -\frac{j}{w^2} \left\{ j \frac{\beta \nu}{r} C_1 K_\nu(wr) - \omega \mu w D_1 K'_\nu(wr) \right\} e^{j(\omega t - \beta z + \nu \phi)} \quad (4a)$$

$$H_{\phi 2} = -\frac{j}{u^2} \left\{ \omega \varepsilon w C_1 K'_\nu(wr) + j \frac{\beta \nu}{r} D_1 K_\nu(wr) \right\} e^{j(\omega t - \beta z + \nu \phi)} \quad (4b)$$

In these equations, the subscripts 1 and 2, respectively, indicate the situations in the core and the clad sections, ε and μ , respectively, represent the permittivity and the permeability of fiber mediums, and A_1 , B_1 , C_1 and D_1 are unknown constants to be determined by the boundary conditions. Also, the parameters u and w are, respectively, defined as $u = \sqrt{(n_1 k_0)^2 - \beta^2}$ and $w = \sqrt{\beta^2 - (n_2 k_0)^2}$ with β as the axial propagation constant and k as the free-space propagation constant. Further, $J_\nu(\bullet)$ and $K_\nu(\bullet)$, respectively, represent Bessel and the modified Bessel functions [26]. Now, these field equations can be treated under the use of suitable boundary conditions, as discussed in Ref. [25], to obtain the dispersion relations of the guide. It is noteworthy that, in the present case of core-clad interface (of optical fiber), the electric field will vanish along the direction of helix pitch, and will remain continuous along the direction perpendicular to the pitch. Further, the tangential components of magnetic field will be continuous at the core-clad interface. Following the procedure in Ref. [19], it can be shown that the dispersion relation of fiber will

assume the general simplified form as

$$\begin{aligned}
 f(\beta) = & J_\nu(au)\Theta \left\{ \frac{K_\nu^2(aw)}{(aw^2)^2} (\nu\beta \cos \psi + aw^2 \sin \psi)^2 - \omega^2 \mu \varepsilon \Xi^2 \right\} \cos^2 \psi \\
 & + \frac{\omega^2 \mu \varepsilon}{4} K_\nu(aw) \Theta^2 \Xi (\sin^2 \psi - \cos^2 \psi) \cos^2 \psi \\
 & + J_\nu^2(au) K_\nu(aw) \Xi \left(\sin \psi + \frac{\nu\beta \cos \psi}{au^2} \right) (\cos^2 \psi - \sin^2 \psi) = 0 \quad (5)
 \end{aligned}$$

where $\Xi = K_{\nu-1}(aw) + K_{\nu+1}(aw)$ and $\Theta = J_{\nu-1}(au) - J_{\nu+1}(au)$.

A proper treatment of electromagnetic fields (in Eqs. (1), (2), (3) and (4)) in the fiber will provide the energy flux densities [27] in the core (S_{zc}) and clad (S_{zcl}) sections, as stated below:

$$\begin{aligned}
 S_{zc} = & \frac{\beta\omega}{2\mu^4} (\varepsilon |A_1|^2 + \mu |B_1|^2) \left\{ \left(\frac{\nu}{r} \right)^2 J_\nu^2(ur) \right. \\
 & \left. + \left(\frac{u}{2} \right)^2 (\Phi - 2J_{\nu-1}(ur)J_{\nu+1}(ur)) \right\} \quad (6)
 \end{aligned}$$

$$\begin{aligned}
 S_{zcl} = & \frac{\beta\omega}{2w^4} (\varepsilon |C_1|^2 + \mu |D_1|^2) \left\{ \left(\frac{\nu}{r} \right)^2 K_\nu^2(wr) \right. \\
 & \left. + \left(\frac{w}{2} \right)^2 (\Omega - 2K_{\nu-1}(wr)K_{\nu+1}(wr)) \right\} \quad (7)
 \end{aligned}$$

with $\Phi = J_{\nu-1}^2(ur) + J_{\nu+1}^2(ur)$ and $\Omega = K_{\nu-1}^2(wr) + K_{\nu+1}^2(wr)$.

It can be shown that the unknown constants B_1 , C_1 and D_1 are finally obtained in terms of the constant A_1 , as follows:

$$B_1 = A_1 \frac{jJ_\nu(ua) (u^2a \sin \psi + \beta\nu \cos \psi)}{\omega\mu au J'_\nu(ua) \cos \psi} \quad (8)$$

$$C_1 = A_1 \frac{w^3 (L \cos \psi + M \sin \psi)}{u^2 K_\nu(aw) \{w^2 a N + \beta\nu P \sin \psi\} \cos \psi} \quad (9)$$

$$D_1 = A_1 \frac{jw^2 Q (L \cos \psi + uM \sin \psi)}{u^2 K_\nu(aw) \{w^2 a N + \beta\nu P \sin \psi\} \cos^2 \psi} \quad (10)$$

with $L = J_\nu(ua)\{u^2a \cos \psi - \beta\nu \sin \psi\}$, $M = J_\nu(ua)\{u^2a \sin \psi - \beta\nu \cos \psi\}$, $N = j\omega\mu a K'_\nu(wa) \sin^2 \psi - w \cos \psi$, $P = j\omega\mu a K'_\nu(wa) \sin \psi - w \cos^2 \psi$, and $Q = j\omega\mu a K'_\nu(wa) \sin \psi - \beta\nu K_\nu(wa)$.

3. RESULTS AND DISCUSSION

We now make an attempt to investigate the propagation patterns of flux density into the fiber, which is considered to be bounded with

right-handed conducting sheath helix at the core-clad interface. In this stream, flux densities corresponding to the two low order modes EH_{11} and EH_{12} are given attention under the situation of helix pitch as 0° , 45° and 90° . For this purpose, we consider the operating wavelength to be $1.55 \mu\text{m}$, and the different values of core radius as $10 \mu\text{m}$, $20 \mu\text{m}$ and $50 \mu\text{m}$ along with the assumption of the guide to have an infinitely extended clad. Also, the RIs values are taken as $n_1 = 1.49$ and $n_2 = 1.47$. In order to obtain the propagation constants corresponding to the aforesaid modes, the eigenvalue Eq. (5) is used. The corresponding plots are, however, not included into the text. But, Table 1 states the allowed values of propagation constants under the use of above mentioned dimensional values of the guide, as estimated for EH_{11} and EH_{12} modes corresponding to 0° , 45° and 90° helix pitch; these are evaluated by the use of dispersion relation Eq. (5).

Figures 2–6 illustrate the flux density characteristics in the core/clad sections of twisted clad fiber considering three different

Table 1. Allowed values of propagation constant β .

Helix pitch angle ψ	Modes	Core radius a (in μm)	Propagation constant β (in m^{-1})
0°	EH_{11}	10	5.960×10^6
	EH_{12}	10	5.990×10^6
	EH_{11}	20	5.973×10^6
	EH_{12}	20	5.964×10^6
	EH_{11}	50	5.982×10^6
	EH_{12}	50	5.985×10^6
45°	EH_{11}	10	6.001×10^6
	EH_{12}	10	6.002×10^6
	EH_{11}	20	5.978×10^6
	EH_{12}	20	5.976×10^6
	EH_{11}	50	5.978×10^6
	EH_{12}	50	5.977×10^6
90°	EH_{11}	10	6.000×10^6
	EH_{12}	10	5.979×10^6
	EH_{11}	20	5.970×10^6
	EH_{12}	20	5.972×10^6
	EH_{11}	50	5.980×10^6
	EH_{12}	50	5.984×10^6

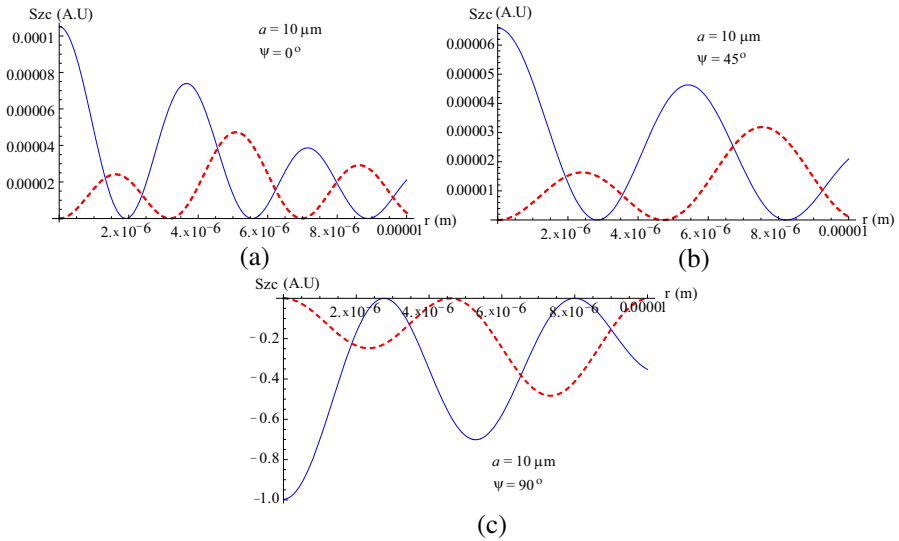


Figure 2. Flux density in the fiber core corresponding to $a = 10 \mu\text{m}$ and (a) $\psi = 0^\circ$, (b) $\psi = 45^\circ$ and (c) $\psi = 90^\circ$.

dimensional as well as pitch angle values, as stated above. In these figures, solid and dashed lines, respectively, correspond to the situations of EH_{11} and EH_{12} modes.

Considering the fiber radius as $10 \mu\text{m}$, Fig. 2 depicts the patterns of flux density in the fiber core, whereas those in the clad region are shown in Fig. 3. We observe from Fig. 2 that, corresponding to all pitch angles of the loaded conducting sheath helix, flux exhibits oscillatory trend, and decreases as the core-clad interface is reached. Comparing Figs. 2(a), 2(b) and 2(c), we observe that, corresponding to the EH_{11} mode, the flux density is mostly confined near the central region of the fiber core, which is in contrast to the case of EH_{12} mode as it shows the minimum flux at the fiber center. Also, for all pitch angles, the EH_{11} mode shows larger average value of flux density than the higher order EH_{12} mode. This characteristic is repeated for all the chosen angles of helix pitch, and the average value of flux decreases with increasing radial parameter. The higher value of flux corresponding to the EH_{11} is justified as the higher order EH_{12} mode will essentially lose some amount of energy due to the dispersion mechanism. The maximum confinement of flux in the central region is achieved corresponding to the case of 0° pitch, and it is seen to be positive for 0° and 45° values of helix pitch. Corresponding to 90° pitch angle, we observe that EH_{11} and EH_{12} both exhibit negative values of flux density. All these features indicate that the loaded sheath helix plays greatly important role in governing the dispersion characteristics of fiber.

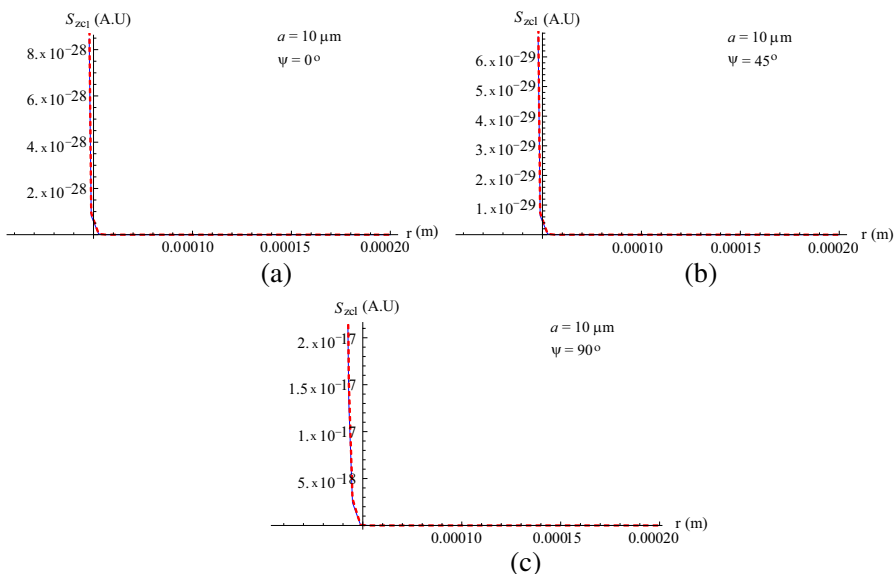


Figure 3. Flux density in the fiber clad corresponding to $a = 10 \mu\text{m}$ and (a) $\psi = 0^\circ$, (b) $\psi = 45^\circ$ and (c) $\psi = 90^\circ$.

For the same fiber dimension, we observe from Fig. 3 that the flux density in the clad section remains extremely small as compared to that in the core region. For all the three values of chosen helix pitch angles, the EH_{11} and EH_{12} modes both exhibit almost similar trends of flux (Figs. 3(a), 3(b) and 3(c)) — it is a little higher near the core-clad interface, and then becomes almost zero with increasing radial parameter. We observe that the flux density in the clad section is maximum corresponding to 90° pitch angle (Fig. 3(c)), i.e., for the parallel orientation of helix with respect to the optical axis, though it is quite negligible as compared to the flux in the fiber core.

An increase of fiber radius to $20 \mu\text{m}$ makes the energy flux density patterns in the fiber core to acquire more oscillatory trend, as can be observed from Fig. 4. This is very much expected as a wider dimension allows more room for the power to propagate. Another noticeable change can be observed corresponding to 45° pitch as the flux confinement due to the EH_{11} mode is slightly increased in the central region of fiber core as compared to the situation of Fig. 2(b). Apart from this, we find the other trends to be similarly to what has been observed in the case of $10 \mu\text{m}$ core radius. These include the oscillatory trend of flux density patterns for the EH_{11} and EH_{12} modes, the EH_{11} mode to have more confined flux in the central region of the fiber, and the negative flux density for the EH_{11} and EH_{12} modes

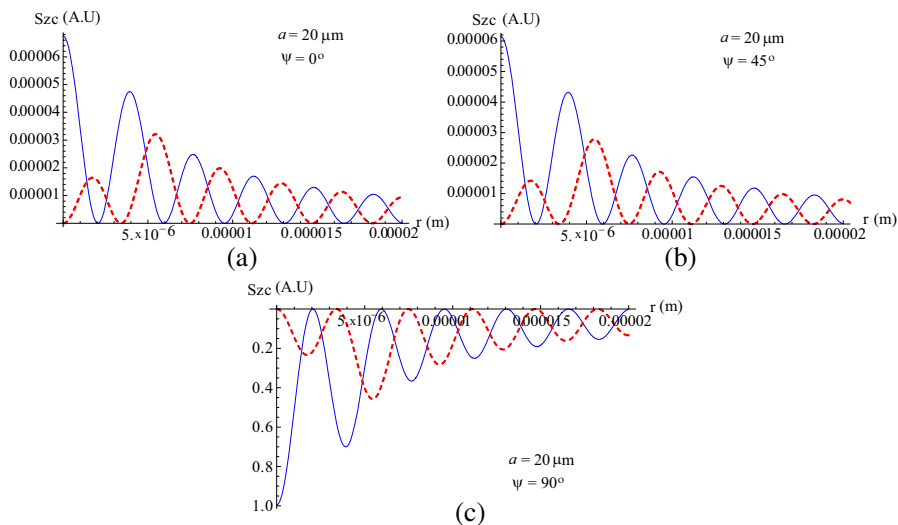


Figure 4. Flux density in the fiber core corresponding to $a = 20 \mu\text{m}$ and (a) $\psi = 0^\circ$, (b) $\psi = 45^\circ$ and (c) $\psi = 90^\circ$.

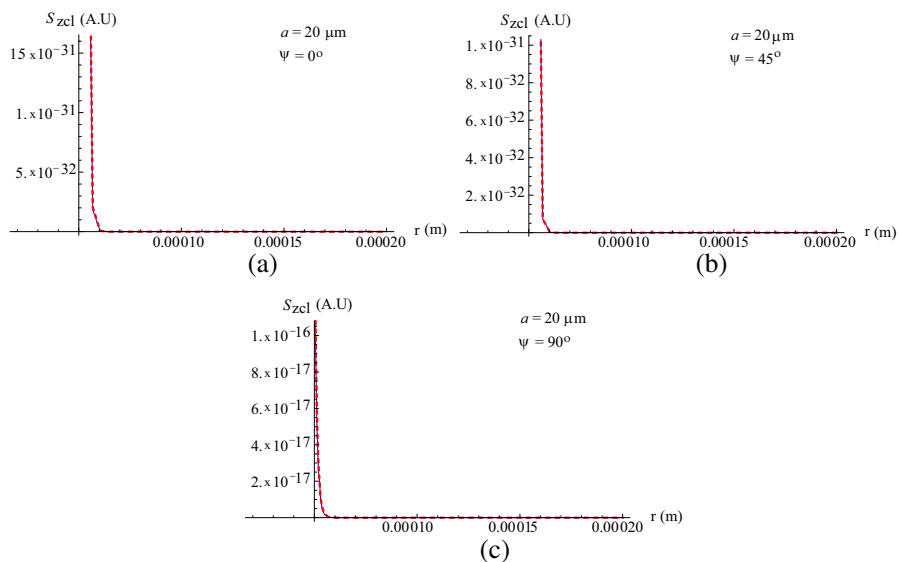


Figure 5. Flux density in the fiber clad corresponding to $a = 20 \mu\text{m}$ and (a) $\psi = 0^\circ$, (b) $\psi = 45^\circ$ and (c) $\psi = 90^\circ$.

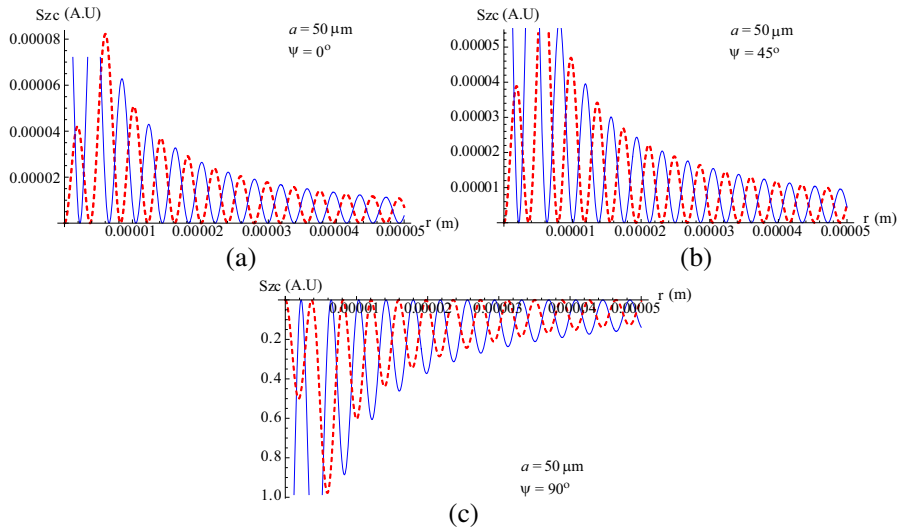


Figure 6. Flux density in the fiber core corresponding to $a = 50 \mu\text{m}$ and (a) $\psi = 0^\circ$, (b) $\psi = 45^\circ$ and (c) $\psi = 90^\circ$.

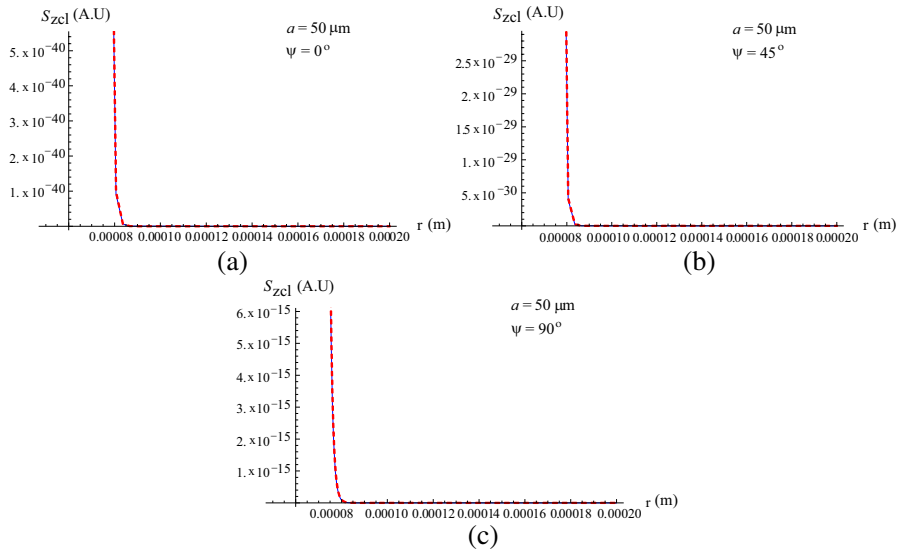


Figure 7. Flux density in the fiber clad corresponding to $a = 50 \mu\text{m}$ and (a) $\psi = 0^\circ$, (b) $\psi = 45^\circ$ and (c) $\psi = 90^\circ$.

corresponding to the case of 90° helix pitch. Fig. 5 indicates the similar (to the case of Fig. 3) trends of flux density in the fiber clad too except the fact that it is further reduced in this case, as compared to what

has been observed in Fig. 3. Otherwise, for all the three values of pitch angles, both the EH_{11} and EH_{12} modes show exactly similar trend as noticed before — it does have negligibly small values in the neighborhood of core-clad interface, and vanishes with the increase in radial parameter.

A further increase of radial dimension to $50\ \mu\text{m}$ brings in prime changes in flux density patterns in respect of the more oscillatory behavior of those, as can be observed in Fig. 6. We notice that flux due to both the EH_{11} and EH_{12} modes exhibit more dense oscillations, which is essentially owing to the allowance of the sustained modes to have more rooms while propagating; flux decreases with increasing radial direction, and the case of 90° helix pitch angle exhibits negative flux. In the clad section, the flux density is further reduced near the core-clad boundary (Fig. 7) as compared to the situations in Figs. 3 and 5. Apart from this, the other trends are almost similar to what observed in respect of lower fiber dimensions.

4. CONCLUSION

From the foregoing discussions, inference can be drawn that the loading of conducting sheath helix at the core-clad interface brings in alterations in the dispersion properties of fiber. Studies have been made considering a few values of helix pitch angles as well as fiber dimensions. It has been found that the propagation of flux density is greatly governed by the introduced helix pitch. As such, the propagation features of these guides can be tailored on demand, which would find potential optical applications.

ACKNOWLEDGMENT

This work is partially supported by the Fundamental Research Grant Project (FRGS/1/2011/TK/UKM/01/16) by the Ministry of Higher Education (Malaysia); the authors are thankful to the Ministry. The authors are thankful to the anonymous reviewer for constructive criticisms on the text of the manuscript, which essentially helped to improve its status.

REFERENCES

1. Choudhury, P. K. and O. N. Singh, "Some multilayered and other unconventional lightguides," *Electromagnetic Fields in Unconventional Structures and Materials*, O. N. Singh and A. Lakhtakia, Eds., 289–357, Wiley, USA, 2000.

2. Choudhury, P. K. and T. Yoshino, "Characterization of optical power confinement in a simple chirofiber," *Optik*, Vol. 13, 89–95, 2002.
3. Choudhury, P. K. and T. Yoshino, "A rigorous analysis of the power distribution in plastic clad annular core optical fibers," *Optik*, Vol. 113, 481–488, 2002.
4. Cheng, S. F. and L. K. Chau, "Colloidal gold-modified optical fiber for chemical and biochemical sensing," *Anal. Chem.*, Vol. 75, 16–21, 2003.
5. Nair, A. and P. K. Choudhury, "On the analysis of field patterns in chirofibers," *Journal of Electromagnetic Waves and Applications*, Vol. 21, No. 15, 2277–2286, 2007.
6. Choudhury, P. K. and D. Kumar, "Towards dispersion relations for tapered core dielectric elliptical fibers," *Optik*, Vol. 118, 340–344, 2007.
7. Yeh, C. and I. F. Shimabukuro, *The Essence of Dielectric Waveguides*, Springer, New York, 2008.
8. Choudhury, P. K. and W. K. Soon, "TE mode propagation through tapered core liquid crystal optical fibers," *Progress In Electromagnetics Research*, Vol. 104, 449–463, 2010.
9. Amin, A. S. N., M. Mirhosseini, and M. Shahabadi, "Modal analysis of multilayer conical dielectric waveguides for azimuthal invariant modes," *Progress In Electromagnetics Research*, Vol. 105, 213–229, 2010.
10. Duan, Z., Y. Wang, X. Mao, W.-X. Wang, and M. Chen, "Experimental demonstration of double-negative metamaterials partially filled in a circular waveguide," *Progress In Electromagnetics Research*, Vol. 121, 215–224, 2011.
11. Kesari, V. and J. P. Keshari, "Analysis of a circular waveguide loaded with dielectric and metal discs," *Progress In Electromagnetics Research*, Vol. 111, 253–269, 2011.
12. Choudhury, P. K., "Dispersion behavior of gold-nanocoated dielectric optical fibers," *Adv. in Mat. Sci. Eng.*, Vol. 2012, Article ID 214614, 1–7, 2012.
13. Baqir, M. A. and P. K. Choudhury, "On the energy flux through a uniaxial chiral metamaterial made circular waveguide under PMC boundary," *Journal of Electromagnetic Waves and Applications*, Vol. 26, No. 16, 2165–2175, 2012.
14. Zarifi, D., A. Abdolali, M. Soleimani, and V. Nayyeri, "Inhomogeneous planar layered chiral media: Analysis of wave propagation and scattering using Taylor's series expansion,"

- Progress In Electromagnetics Research*, Vol. 125, 119–135, 2012.
15. Choudhury, P. K., “Evanescence field enhancement in liquid crystal optical fibers — A field characteristics based analysis,” *Adv. in Condensed Mat. Phys.*, Vol. 2013, Article ID 504868, 1–9, 2013.
 16. Dong, J. and J. Li, “Characteristics of guided modes in uniaxial chiral circular waveguides,” *Progress In Electromagnetics Research*, Vol. 124, 331–345, 2012.
 17. Baqir, M. A. and P. K. Choudhury, “Propagation through uniaxial anisotropic chiral waveguide under DB-boundary conditions,” *Journal of Electromagnetic Waves and Applications*, Vol. 27, No. 6, 783–793, 2013.
 18. Singh, U. N., O. N. Singh II, P. Khastgir, and K. K. Dey, “Dispersion characteristics of a helically clad step-index optical fiber: An analytical study,” *J. Opt. Soc. Am. B*, Vol. 12, 1273–1278, 1995.
 19. Kumar, D. and O. N. Singh, II, “Modal characteristic equation and dispersion curves for an elliptical step-index fiber with a conducting helical winding on the core cladding boundary: An analytical study,” *J. Light. Tech.*, Vol. 20, 1416–1424, 2002.
 20. Kumar, D., P. K. Choudhury, and F. A. Rahman, “Low eccentricity elliptical fibers with helical windings under slow-wave consideration — Some special cases,” *Optik*, Vol. 121, 926–933, 2010.
 21. Pierce, J. R., *Travelling Wave Tubes*, D. Van Nostrand, NJ, 1950.
 22. Lim, K. Y., P. K. Choudhury, and Z. Yusoff, “Chirofibers with helical windings — An analytical investigation,” *Optik*, Vol. 121, 980–987, 2010.
 23. Choudhury, P. K., “Transmission through twisted clad liquid crystal optical fibers,” *Progress In Electromagnetics Research*, Vol. 131, 169–184, 2012.
 24. Kumar, D., P. K. Choudhury, and O. N. Singh, II, “Towards the dispersion relations for dielectric optical fibers with helical windings under slow- and fast-wave considerations — A comparative analysis,” *Progress In Electromagnetics Research*, Vol. 80, 409–420, 2008.
 25. Abramowitz, A. and I. A. Stegun, *Handbook of Mathematical Functions*, Dover, New York, 1970.
 26. Adams, M. J., *An Introduction to Optical Waveguides*, 250–257, Wiley, UK, 1981.
 27. Cherin, A. H., *An Introduction to Optical Fibers*, Chapt. 2, McGraw-Hill, New York, 1987.